

## SUPPORTING MATERIAL

### Exploring the Stability Limits of Actin and its Suprastructures

Christopher Rosin,<sup>\*</sup> Mirko Erkamp,<sup>\*</sup> Julian von der Ecken,<sup>†</sup> Stefan Raunser,<sup>†</sup> and Roland Winter<sup>\*</sup>

<sup>\*</sup>TU Dortmund University, Department of Chemistry and Chemical Biology, Physical Chemistry I - Biophysical Chemistry, D-44227 Dortmund, Germany; and <sup>†</sup>Max Planck Institute of Molecular Physiology, Department of Structural Biochemistry, D-44227 Dortmund, Germany

#### Additional results

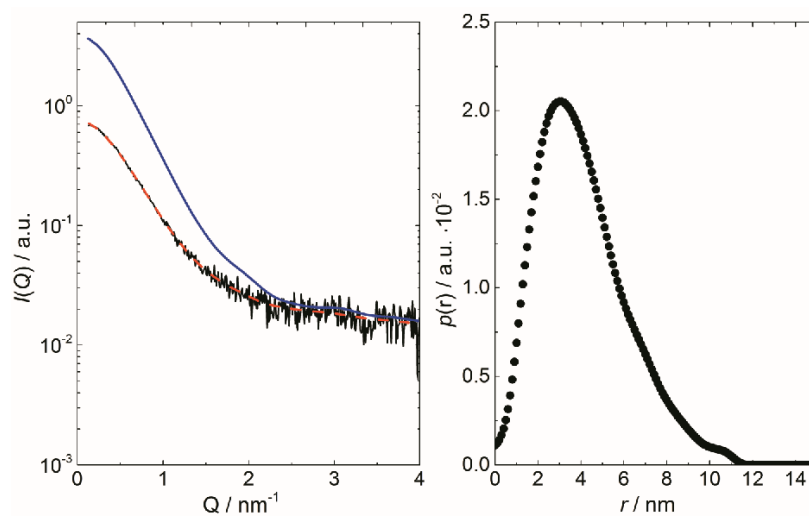


**Fig. S 1.** Left: SAXS data,  $I(Q)$ , of TMR-G-actin,  $10 \text{ mg mL}^{-1}$ , at 298 K. The raw data and the fit are represented by the black and red curves, respectively. The blue curve has been obtained after correction for line focus (desmearing) and background. Right: Distance distribution function,  $p(r)$ , of TMR-G-actin.

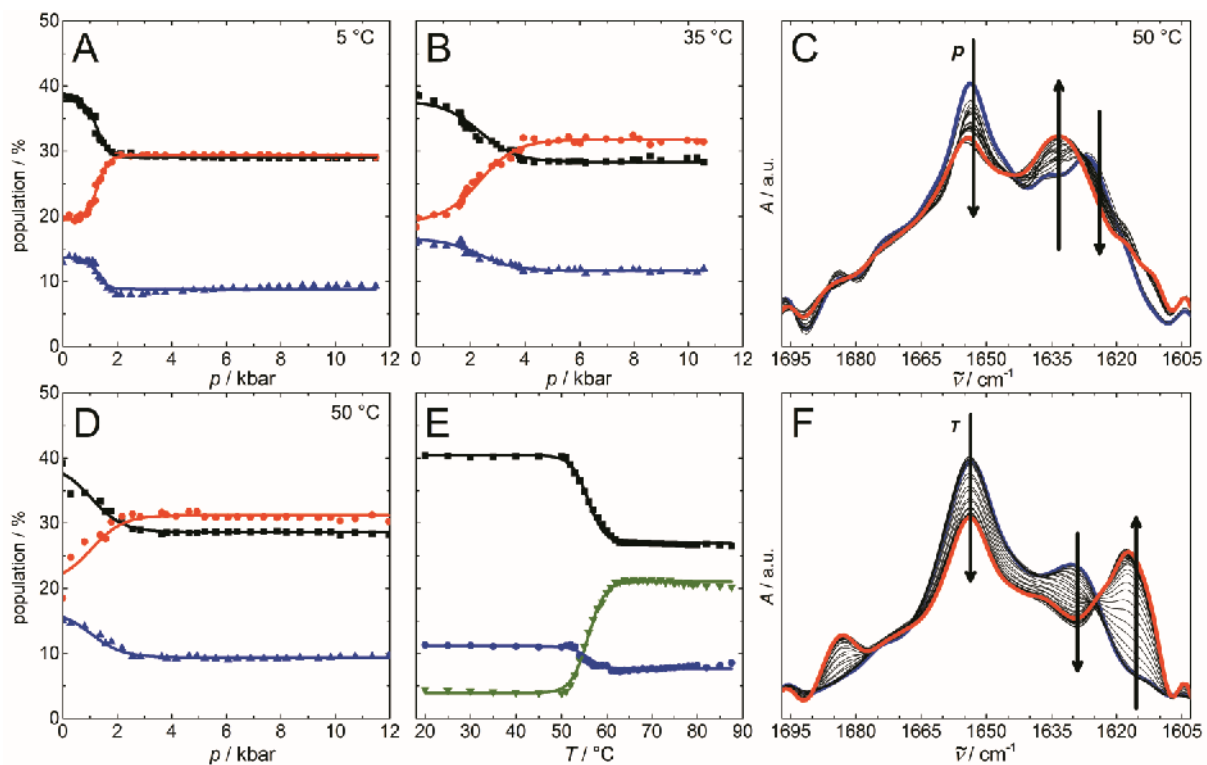


**Fig. S 2.** Temperature and pressure dependent FTIR data on G-actin. Example of pressure (at  $T = 50\text{ }^{\circ}\text{C}$ , C) and temperature (at  $p = 1\text{ bar}$ , F) dependent changes in the deconvoluted absorption signal of the amide I' band. Changes in secondary structure elements by pressure at selected temperatures (A, B, D), and of temperature dependent changes at ambient pressure (E). Lines are Boltzmann fits to the experimental data using Eqs. 1, 2. (■  $\alpha$ -helix ( $1655\text{ cm}^{-1}$ ) ● intramolecular  $\beta$ -sheets ( $1635\text{ cm}^{-1}$ ) ▲ intramolecular  $\beta$ -sheets ( $1627\text{ cm}^{-1}$ ) ▼ intermolecular  $\beta$ -sheets ( $1616\text{ cm}^{-1}$ )).

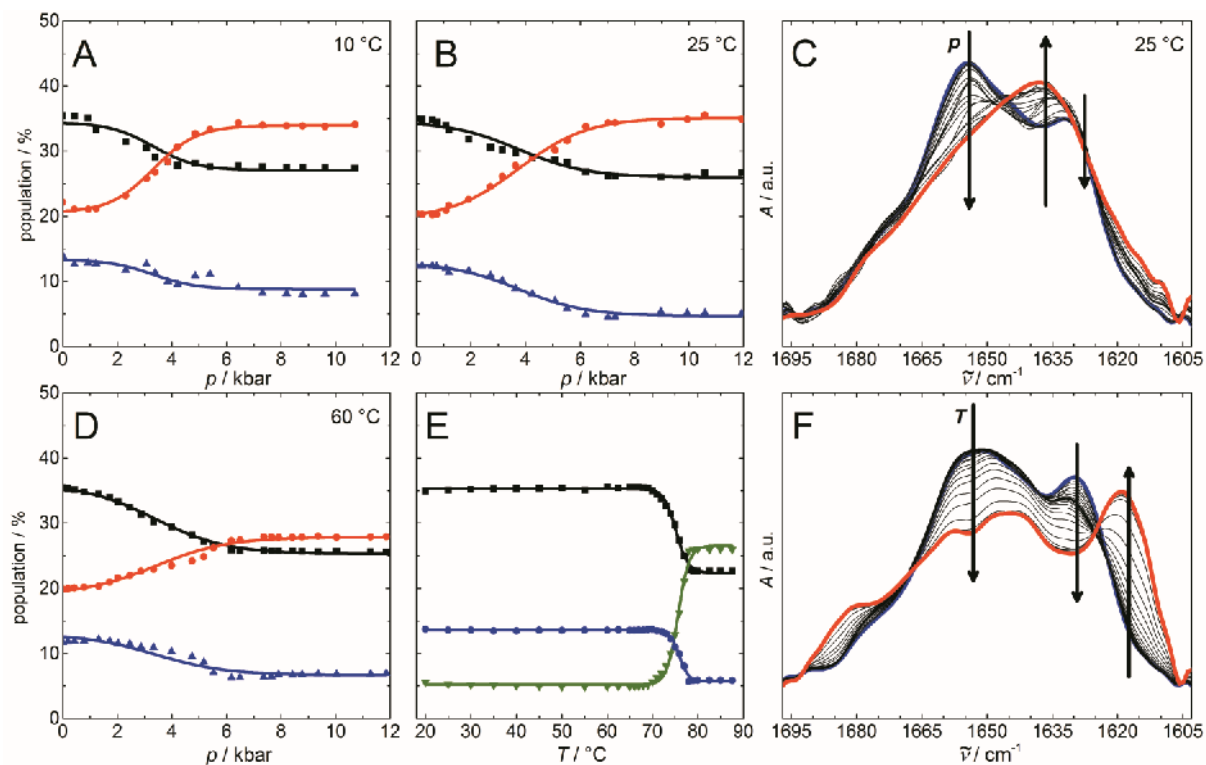


**Fig. S 3.** Temperature and pressure dependent FTIR data on F-actin. Example of pressure (at  $T = 25\text{ }^{\circ}\text{C}$ , C) and temperature (at  $p = 1\text{ bar}$ , F) dependent changes in the deconvoluted absorption signal of the amide I' band. Changes in secondary structure elements by pressure at selected temperatures (A, B, D), and of temperature dependent changes at ambient pressure (E). Lines are Boltzmann fits to the experimental data using Eqs. 1, 2. (■  $\alpha$ -helix ( $1655\text{ cm}^{-1}$ ) ● intramolecular  $\beta$ -sheets ( $1635\text{ cm}^{-1}$ ) ▲ intramolecular  $\beta$ -sheets ( $1627\text{ cm}^{-1}$ ) ▼ intermolecular  $\beta$ -sheets ( $1616\text{ cm}^{-1}$ )).

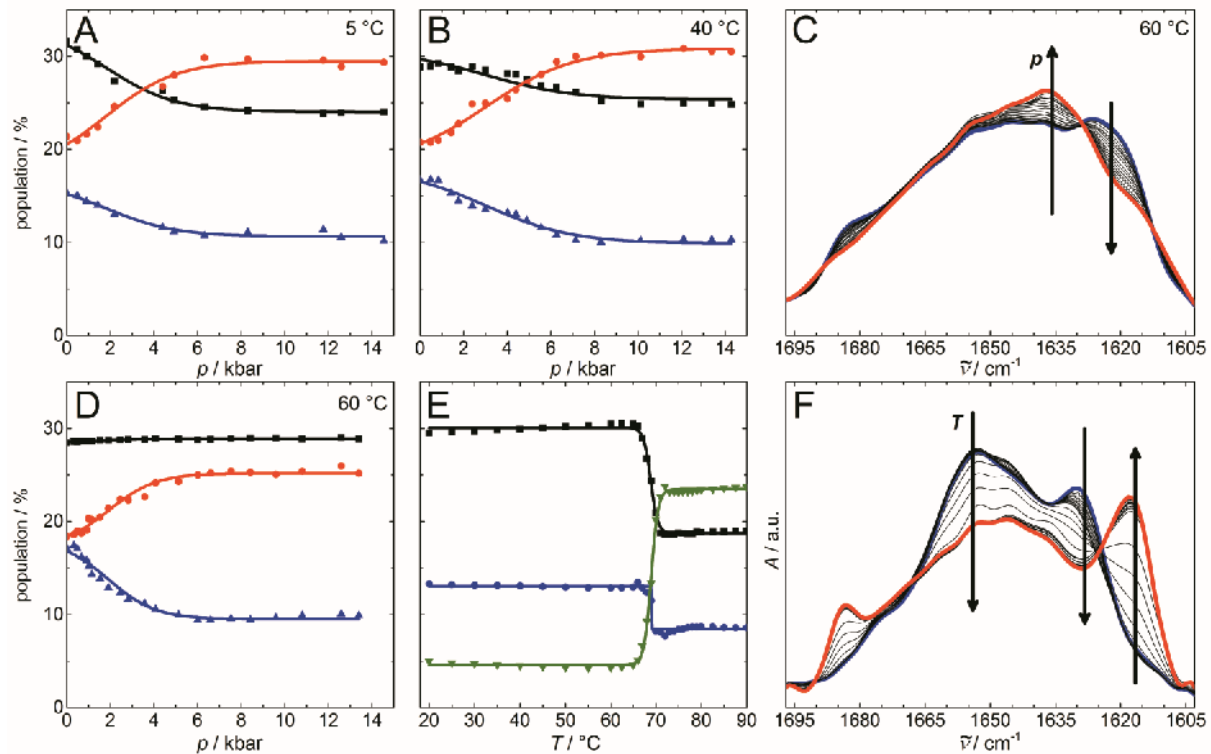


**Fig. S 4.** Temperature and pressure dependent FTIR data on B-actin. Example of pressure (at  $T = 60\text{ }^{\circ}\text{C}$ , C) and temperature (at  $p = 1\text{ bar}$ , F) dependent changes in the deconvoluted absorption signal of the amide I' band. Changes in secondary structure elements by pressure at selected temperatures (A, B, D), and of temperature dependent changes at ambient pressure (E). Lines are Boltzmann fits to the experimental data using Eqs. 1, 2. (■  $\alpha$ -helix ( $1655\text{ cm}^{-1}$ ) ● intramolecular  $\beta$ -sheets ( $1635\text{ cm}^{-1}$ ) ▲ intramolecular  $\beta$ -sheets ( $1627\text{ cm}^{-1}$ ) ▼ intermolecular  $\beta$ -sheets ( $1616\text{ cm}^{-1}$ )).

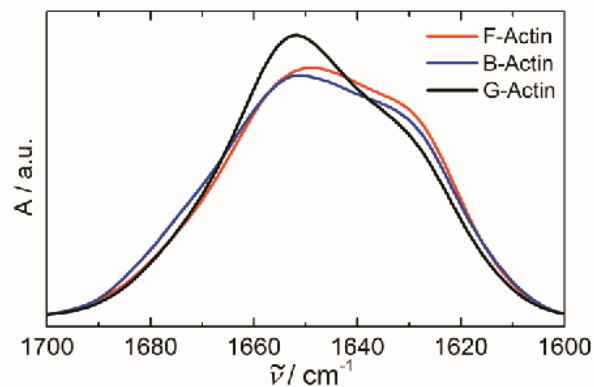


**Fig. S 5.** Comparison of normalized amide I' bands of G-, B- and F-actin at  $20\text{ }^{\circ}\text{C}$ . The amide I' bands of the different actin species show differences in the composition of secondary structure elements, in particular between G- and B-/F-actin.

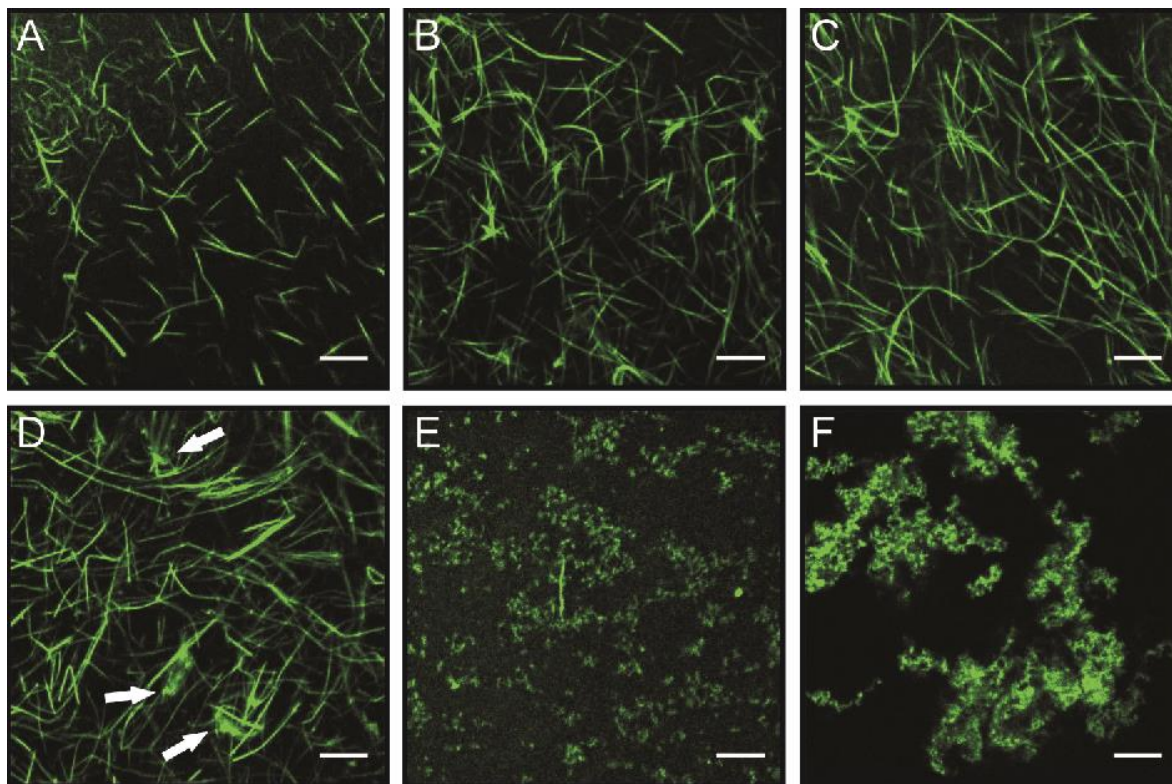


**Fig. S 6.** LCMS microscopy of pressurized/heated actin bundles. Bundled actin was subjected to different pressures (for 20 min) followed by decompression and staining with phalloidin. (A) LCMS images of B-actin at 1 bar, after pressurization up to 1.5 kbar (B), 2.5 kbar (C), 3.5 kbar (D) and 5 kbar (E). To visualize also the effect of temperature-induced aggregation, the sample was heated to 90 °C for 20 min (F). Scale bar: 10  $\mu$ m. Arrows indicate first dissociated bundles, which aggregate into small assemblies at 3.5 kbar. LCMS measurements of pressure/temperature treated actin bundles are in good agreement with the results of our TEM studies (see Figure 7).

**Table S 1.** IR band assignment of the different subbands of actin in the amide I' band region (1).

Secondary structural element	Amide I' band region / $\text{cm}^{-1}$
side chains	< 1615
intermolecular $\beta$ -sheets	~1615, ~1684
intramolecular $\beta$ -sheets	~1627, ~1635
disordered structures	~1643
$\alpha$ -helix	~1655
loops / turns	~1660-1670

**Table S 2.** Thermodynamic data of the unfolding transition of G-actin, F-actin and B-actin as obtained from the DSC, PPC and FTIR spectroscopic data.

Parameter	G-actin	B-actin	F-actin
$T_m / ^\circ\text{C}$ (FTIR)	$56.0 \pm 2$	$68.9 \pm 2$	$75.5 \pm 2$
$T_m / ^\circ\text{C}$ (DSC)	$56.8 / 60.4 \pm 1$	$70.8 / 72.2 / 73.7 \pm 1$	$73.8 / 75.2 / 75.7 \pm 1$
Thermal unfolding	biphasic	triphasic	triphasic
$\Delta H_{\text{vH}} / \text{kJ mol}^{-1}$	$483 \pm 101$	$1120 \pm 175$	$821 \pm 141$
$\Delta H_{\text{cal}} / \text{kJ mol}^{-1}$	$364 \pm 34$	$946 \pm 65$	$874 \pm 36$
$\Delta V(25^\circ\text{C}, p) / \text{mL mol}^{-1}$	$-16 \pm 6$	$-9 \pm 6$	$-20 \pm 11$
$\Delta V(T_m, 1\text{bar}) / \text{mL mol}^{-1}$	-36	34	26
$p_u(25^\circ\text{C}) / \text{kbar}$	$2.2 \pm 0.15$	$2.7 \pm 0.15$	$3.8 \pm 0.15$

$T / ^\circ\text{C}$	$\Delta V(T)$ G-actin / $\text{mL mol}^{-1}$	$\Delta V(T)$ B-actin / $\text{mL mol}^{-1}$	$\Delta V(T)$ F-actin / $\text{mL mol}^{-1}$
5	$-11 \pm 9$	$-14 \pm 9$	-
10	-	-	$-29 \pm 14$
20	$-16 \pm 6$	-	$-21 \pm 7$
25	-	$-9 \pm 6$	$-20 \pm 11$
35	$-35 \pm 8$	-	-
40	-	$-13 \pm 6$	$-14 \pm 8$
50	$-45 \pm 13$	-	-
60	-	$-26 \pm 7$	$-21 \pm 5$

## Supporting References

1. Byler, M., and H. Susi. (1986). Examination of the Secondary Structure of Proteins by Deconvolved FTIR Spectra. *Biopolymers*. 25, 469–487.